

Chiral 3π -exchange NN-potentials: results for representation-invariant classes of diagrams

N. Kaiser

Physik Department T39, Technische Universität München,
D-85747 Garching, Germany

Abstract

We calculate in (two-loop) chiral perturbation theory the local NN-potentials generated by certain classes of three-pion exchange diagrams. We stress that the chiral $3\pi NN$ -contact vertex depends on the particular choice of the interpolating pion-field and therefore one has to consider representation invariant classes of diagrams by supplementing graphs involving the chiral 4π -vertex. We find that the resulting isovector spin-spin and tensor NN-potentials are negligibly small for $r \geq 0.8$ fm. One can conclude that the effects of uncorrelated chiral 3π -exchange in the NN-interaction are very small and therefore of no practical relevance.

PACS: 12.20.Ds, 12.38.Bx, 12.39.Fe, 13.75.Cs.

Accepted for publication in: *Physical Review C*

The longest-range part of the strong nucleon-nucleon interaction is due to the well-established one-pion exchange. Next in range comes the two-pion exchange force, whose formulation has been a longstanding problem in quantum field theory and in dispersion theory. In recent years, it has been argued that the key to the solution is the chiral symmetry of QCD, and that the long-range parts of the two-pion exchange NN-potential can be derived model-independently via a systematic expansion of the effective chiral pion-nucleon Lagrangian. The complete leading and next-to-leading order terms of this chiral two-pion exchange NN-potential have been calculated in ref.[1] (actually most of the contributions have already been obtained in earlier calculations). Recently, the elastic proton-proton scattering data base below 350 MeV laboratory kinetic energy (consisting of 1951 data points) has been analyzed in terms of one-pion exchange and chiral two-pion exchange in ref.[2]. The resulting good $\chi^2/dof \leq 1$ constitutes a convincing proof for the presence of the chiral two-pion exchange in the long-range proton-proton strong interaction. Furthermore, it was concluded in ref.[2] that 1π -exchange together with chiral 2π -exchange gives a very good NN-force at least as far inwards as $r = 1.4$ fm inter-nucleon distance.

Naturally, the next question to be answered is whether there are some important effects from chiral three-pion exchange. In a recent work Pupin and Robilotta [3] calculated the potentials generated by one specific two-loop diagram in which the three pions are emitted from a contact vertex at the first nucleon and absorbed on a contact vertex at the second nucleon (first graph in Fig. 1). The resulting isovector spin-spin and tensor potentials were

rather small with values of less than 1.6 MeV for distances $r \geq 0.8$ fm, i.e. two to three orders of magnitude smaller than typical 2π -exchange potentials. The form of the chiral $3\pi NN$ -contact vertex employed in the calculation of ref.[3] stems from an effective chiral Lagrangian using a specific choice of the interpolating pion-field. As a matter of fact the non-linear realization of chiral symmetry [4] allows for redefinitions of the pion-field and consequently the result of the single diagram studied in ref.[3] becomes non-unique. On the level of Feynman diagrams this feature implies that only suitable classes of graphs, but not individual diagrams can have a physical meaning. This fact was also stressed in ref.[5] when calculating the isoscalar central NN-amplitude generated by correlated chiral 2π -exchange. The diagram involving the chiral 4π -vertex had to be supplemented by four additional graphs involving the chiral $3\pi NN$ -contact vertex. The purpose of this work is to present results for the chiral 3π -exchange NN-potential as given by such complete classes of diagrams. A calculation of the very large number of all possible (two-loop) 3π -exchange diagrams goes beyond the scope of the present short paper. In order to learn about the generic size of uncorrelated 3π -exchange effects in the NN-interaction we will restrict ourselves here to the evaluation of four (relatively simple) classes of diagrams. In fact these four classes comprise all 3π -exchange graphs carrying a common prefactor g_A^2/f_π^6 .

Let us begin with recalling the effective chiral Lagrangians for $\pi\pi$ - and πN -interaction, which read at lowest order

$$\mathcal{L}_{\pi\pi}^{(2)} = \frac{f_\pi^2}{4} \text{tr}(\partial^\nu U \partial_\nu U^\dagger + m_\pi^2(U + U^\dagger)), \quad (1)$$

$$\mathcal{L}_{\pi N}^{(1)} = \bar{N} \left(iD_0 - \frac{g_A}{2} \vec{\sigma} \cdot \vec{u} \right) N, \quad u^\nu = i\{\xi^\dagger, \partial^\nu \xi\}, \quad (2)$$

where $f_\pi = 92.4$ MeV is the weak pion decay constant and $g_A = g_{\pi N} f_\pi / M = 1.32$ as given by the Goldberger-Treiman relation together with $g_{\pi N} = 13.4$. The choice $g_A = 1.32$ is most natural in the present context since the pion-nucleon vertex is the relevant one here and not the axial-vector coupling. $\mathcal{L}_{\pi N}^{(1)}$ is presented in the heavy baryon formulation (i.e. a non-relativistic treatment of the nucleons) with $\vec{\sigma}$ denoting the Pauli spin-matrices and $D^\nu = \partial^\nu + \frac{1}{2}[\xi^\dagger, \partial^\nu \xi]$ the chiral covariant derivative acting on the iso-doublet nucleon-field N . The $SU(2)$ -matrix $U = \xi^2$ collects the Goldstone pion-fields in the form

$$U(\vec{\pi}) = 1 + \frac{i}{f_\pi} \vec{\tau} \cdot \vec{\pi} - \frac{1}{2f_\pi^2} \vec{\pi}^2 - \frac{i\alpha}{f_\pi^3} (\vec{\tau} \cdot \vec{\pi})^3 + \frac{8\alpha - 1}{8f_\pi^4} \vec{\pi}^4 + \dots \quad (3)$$

Note that only the coefficients of the linear and quadratic term in the pion-field $\vec{\pi}$ are fixed by the proper normalization of the kinetic term and the unitary condition $U^\dagger U = 1$. The numerical coefficient α in front of the third power of the pion-field is *arbitrary* and it reappears via the unitarity condition $U^\dagger U = 1$ in front of the $\vec{\pi}^4$ -term. In fact, when continuing the power series expansion of $U(\vec{\pi})$ in eq.(3) one encounters an infinite number of arbitrary coefficients. This just reflects the well-known fact that the non-linear realization of chiral symmetry [4] on the pion-fields is unique only up to an arbitrary function $f(\vec{\pi}^2)$. As a consequence of eq.(3) the off-shell 4π -vertex

$$\frac{i}{f_\pi^2} \left\{ \delta^{ab} \delta^{cd} [(q_1 + q_2)^2 - m_\pi^2 + 2\alpha(4m_\pi^2 - q_1^2 - q_2^2 - q_3^2 - q_4^2)] + \text{two cycl. perm.} \right\} \quad (4)$$

and the chiral $3\pi NN$ -vertex (i.e. $N \rightarrow N + \pi^a(q_1) + \pi^b(q_2) + \pi^c(q_3)$),

$$\frac{g_A}{4f_\pi^3} \vec{\sigma} \cdot \left\{ \tau^a \delta^{bc} [4\alpha \vec{q}_1 + (4\alpha - 1)(\vec{q}_2 + \vec{q}_3)] + \text{two cycl. perm.} \right\} \quad (5)$$

both become α -dependent. In (measurable) on-shell matrix elements the unphysical parameter α must of course drop out. For elastic $\pi\pi$ -scattering this is obvious due to the mass-shell condition $q_1^2 = q_2^2 = q_3^2 = q_4^2 = m_\pi^2$. The T-matrix for the reaction $\pi N \rightarrow \pi\pi N$ at threshold in the center-of-mass frame

$$\mathcal{T}_{\text{th}}^{\text{cm}}(\pi^a(\vec{k})N \rightarrow \pi^b\pi^c N) = i \vec{\sigma} \cdot \vec{k} \left[D_1(\tau^b\delta^{ac} + \tau^c\delta^{ab}) + D_2\tau^a\delta^{bc} \right], \quad (6)$$

receives contributions from the chiral $3\pi NN$ -contact vertex eq.(5) and the pion-pole diagram of the form

$$D_1^{\text{cont}} = \frac{g_A}{4f_\pi^3}(4\alpha - 1), \quad D_1^{\pi\text{-pole}} = \frac{g_A}{8f_\pi^3}(3 - 8\alpha), \quad (7)$$

$$D_2^{\text{cont}} = \frac{g_A}{f_\pi^3}\alpha, \quad D_2^{\pi\text{-pole}} = -\frac{g_A}{8f_\pi^3}(8\alpha + 3). \quad (8)$$

The sums $D_{1,2}^{(\text{cont})} + D_{1,2}^{(\pi\text{-pole})}$ are indeed α -independent and they constitute the leading order terms of the chiral low-energy theorems for $\pi N \rightarrow \pi\pi N$ derived in ref.[6]. Note that there is no value of α which would allow one to derive the complete leading order terms for D_1 and D_2 from a single diagram. Graphs with the chiral $3\pi NN$ -contact vertex and graphs with the chiral 4π -vertex always have to be grouped into classes and only the results of such classes of diagrams have a physical meaning.

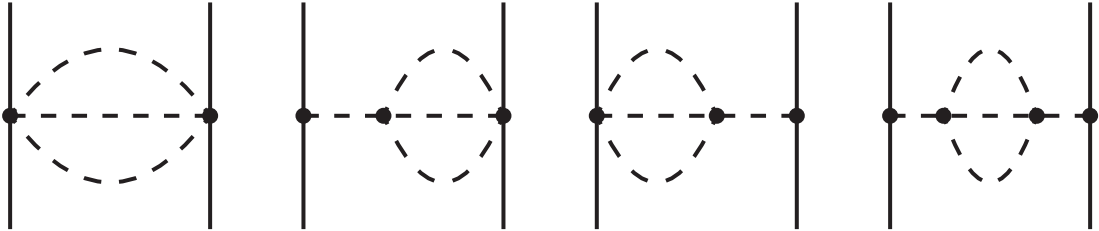


Fig.1: 3π -exchange diagrams of class I. Solid and dashed lines represent nucleons and pions, respectively. The symmetry factor of these graphs is $1/6$.

Let us now turn to the evaluation of (parts of) the chiral 3π -exchange NN-potential. According to the previous discussion the full class of two-loop diagrams shown in Fig.1 should be considered as one entity, whereas in ref.[3] only the first one was evaluated for $\alpha = 0$. From a consideration of the spin- and isospin-factors occurring in these diagrams one finds immediately that only non-vanishing isovector spin-spin and tensor NN-amplitudes will be obtained, i.e. a contribution to the NN T-matrix of the form

$$\mathcal{T}_{NN} = \left[W_S(q) \vec{\sigma}_1 \cdot \vec{\sigma}_2 + W_T(q) \vec{\sigma}_1 \cdot \vec{q} \vec{\sigma}_2 \cdot \vec{q} \right] \vec{\tau}_1 \cdot \vec{\tau}_2, \quad (9)$$

where $q = |\vec{q}|$ denotes the momentum transfer between the initial and final state nucleon. Obviously, the two-loop pion-pole diagrams in Fig.1 contribute via mass and coupling constant renormalization also to the 1π -exchange. These effects are, however, automatically taken care of by working with the physical pion mass m_π and physical πNN -coupling constant $g_{\pi N}$. We are interested here only in the coordinate space potentials generated by the simultaneous exchange of three pions between both nucleons. For that purpose it is sufficient to calculate the imaginary parts of the NN-amplitudes $W_{S,T}(q)$ analytically continued

to time-like momentum transfer $q = i\mu - 0^+$ with $\mu \geq 3m_\pi$. These imaginary parts are then the mass-spectra entering a representation of the local coordinate space potentials in form of a continuous superposition of Yukawa functions,

$$\widetilde{W}_S(r) = \frac{1}{6\pi^2 r} \int_{3m_\pi}^{\infty} d\mu \mu e^{-\mu r} [\mu^2 \text{Im } W_T(i\mu) - 3 \text{Im } W_S(i\mu)], \quad (10)$$

$$\widetilde{W}_T(r) = \frac{1}{6\pi^2 r^3} \int_{3m_\pi}^{\infty} d\mu \mu e^{-\mu r} (3 + 3\mu r + \mu^2 r^2) \text{Im } W_T(i\mu). \quad (11)$$

The spin-spin and tensor potentials, denoted here $\widetilde{W}_{S,T}(r)$, are as usual that ones which are accompanied by the operators $\vec{\sigma}_1 \cdot \vec{\sigma}_2$ and $3\vec{\sigma}_1 \cdot \hat{r} \vec{\sigma}_2 \cdot \hat{r} - \vec{\sigma}_1 \cdot \vec{\sigma}_2$, respectively.

Application of the Cutkosky cutting-rules gives the imaginary parts $\text{Im } W_{S,T}(i\mu)$ as integrals of the squared $\bar{N}N \rightarrow 3\pi$ transition amplitudes over the Lorentz-invariant three-pion phase space. Some details about these techniques can be found in ref.[7] where the method has been used to calculate the spectral-functions of the isoscalar electromagnetic and isovector axial form factors of the nucleon. We find the following result from the diagrams of class I shown in Fig.1,

$$\text{Im } W_S^{(I)}(i\mu) = \frac{g_A^2}{6\mu^4 (16\pi f_\pi^2)^3} \int_{2m_\pi}^{\mu - m_\pi} dw \sqrt{(w^2 - 4m_\pi^2) \lambda^3(w^2, m_\pi^2, \mu^2)}, \quad (12)$$

$$\begin{aligned} \text{Im } W_T^{(I)}(i\mu) &= \frac{2g_A^2 (\mu^2 - m_\pi^2)^{-2}}{9(16\pi f_\pi^2 \mu^2)^3} \int_{2m_\pi}^{\mu - m_\pi} dw \sqrt{(w^2 - 4m_\pi^2) \lambda(w^2, m_\pi^2, \mu^2)} \\ &\times \left[3w^4 (7\mu^4 + 4\mu^2 m_\pi^2 + m_\pi^4) - 2\mu^8 - 19\mu^6 m_\pi^2 - 13\mu^4 m_\pi^4 - 17\mu^2 m_\pi^6 - 3m_\pi^8 \right], \end{aligned} \quad (13)$$

with w the invariant mass of a pion-pair and $\lambda(x, y, z) = x^2 + y^2 + z^2 - 2xy - 2xz - 2yz$ the conventional Källén function. We note that the spin-spin part $\text{Im } W_S^{(I)}(i\mu)$ comes solely from the first graph in Fig.1 independent of the parameter α . In order to compare with the calculation of ref.[3] (i.e. the first diagram in Fig.1 for $\alpha = 0$) one merely has to replace the polynomial in the square bracket of eq.(13) by $(\mu^2 - m_\pi^2)^2 (3w^4 + 10\mu^4 - 5\mu^2 m_\pi^2 - 3m_\pi^4)$. In the chiral limit, $m_\pi = 0$, all integrals can be performed analytically and one obtains 3π -exchange potentials with a simple r^{-7} -dependence,

$$\widetilde{W}_T^{(I)}(r) = 7 \widetilde{W}_S^{(I)}(r) = \frac{70g_A^2}{3(8\pi)^5 f_\pi^6} \frac{1}{r^7}. \quad (14)$$

One observes in the chiral limit that the tensor and spin-spin potentials of the complete class I are a factor 7 and 25 smaller than the ones of ref.[3]. This indicates that there are large cancelations between individual diagrams in class I. The asymptotic fall-off of the coordinate space potentials for $r \rightarrow \infty$ is determined by the behavior of the mass-spectra near the three-pion threshold $\mu = 3m_\pi$. For class I the mass-spectra grow like: $\text{Im } W_S^{(I)}(i\mu) \sim (\mu - 3m_\pi)^3$ and $\text{Im } W_T^{(I)}(i\mu) \sim (\mu - 3m_\pi)^2$, and thus one obtains the following ($r \rightarrow \infty$)-asymptotics

$$\widetilde{W}_T^{(I)}(r) = \widetilde{W}_S^{(I)}(r) = \frac{5g_A^2 m_\pi^3}{3\sqrt{3}(16\pi)^4 f_\pi^6} \frac{e^{-3m_\pi r}}{r^4} + \dots \quad (15)$$

Again, these expressions are a factor 64 smaller than the ones of ref.[3] because of cancelations between different diagrams. Of course, we have recovered all analytical and numerical results of ref.[3] with our method using the corresponding imaginary parts mentioned above.

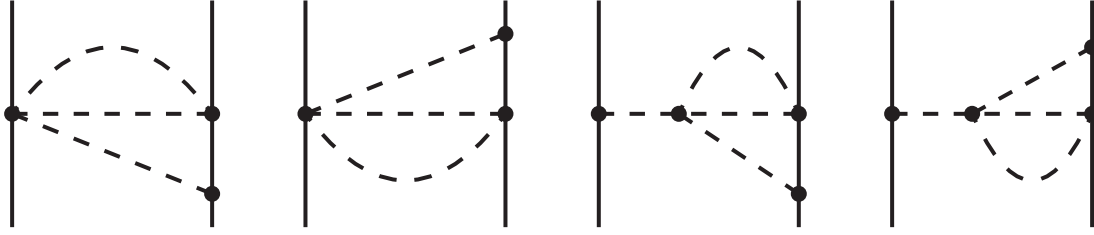


Fig.2: 3π -exchange diagrams of class II. Diagrams for which the role of both nucleons is interchanged are not shown. They lead to the same contribution to the NN-potential. The symmetry factor of these graphs is $1/2$.

Next, we consider the diagrams of class II shown in Fig. 2. These are the diagrams with exactly one nucleon-propagator and because of this property the invariant 3π -phase space integral can still be reduced to a simple one-dimensional integral in the heavy nucleon mass limit $M \rightarrow \infty$ (compare also with $\text{Im } G_A(t)$ in ref.[7]). After a somewhat lengthy calculation we find from class II,

$$\text{Im } W_S^{(II)}(i\mu) = \frac{g_A^2}{3\mu^4(16\pi f_\pi^2)^3} \int_{2m_\pi}^{\mu-m_\pi} dw \sqrt{(w^2 - 4m_\pi^2)\lambda(w^2, m_\pi^2, \mu^2)} w^2(3m_\pi^2 + \mu^2 - 3w^2), \quad (16)$$

$$\begin{aligned} \text{Im } W_T^{(II)}(i\mu) &= \frac{g_A^2}{6(8\pi f_\pi^2 \mu^2)^3} \int_{2m_\pi}^{\mu-m_\pi} dw \sqrt{(w^2 - 4m_\pi^2)\lambda(w^2, m_\pi^2, \mu^2)} \\ &\times \left[w^4 m_\pi^2 (\mu^2 - m_\pi^2)^{-1} - 2w^2 \mu^2 + m_\pi^2 (\mu^2 + m_\pi^2) (3\mu^2 + m_\pi^2) w^{-2} \right]. \end{aligned} \quad (17)$$

In the chiral limit, $m_\pi = 0$, one obtains now attractive isovector tensor and spin-spin potentials with a r^{-7} -dependence,

$$\widetilde{W}_T^{(II)}(r) = \frac{28}{13} \widetilde{W}_S^{(II)}(r) = -\frac{35g_A^2}{18(4\pi)^5 f_\pi^6} \frac{1}{r^7}. \quad (18)$$

The asymptotic fall-off for $r \rightarrow \infty$ differs from class I due to a different threshold behavior of the mass-spectra: $\text{Im } W_S^{(II)}(i\mu) \sim (\mu - 3m_\pi)^4$ and $\text{Im } W_T^{(II)}(i\mu) \sim (\mu - 3m_\pi)^3$, which leads to

$$\widetilde{W}_T^{(II)}(r) = \widetilde{W}_S^{(II)}(r) = -\frac{14g_A^2 m_\pi^2}{3\sqrt{3}(8\pi)^4 f_\pi^6} \frac{e^{-3m_\pi r}}{r^5} + \dots \quad (19)$$

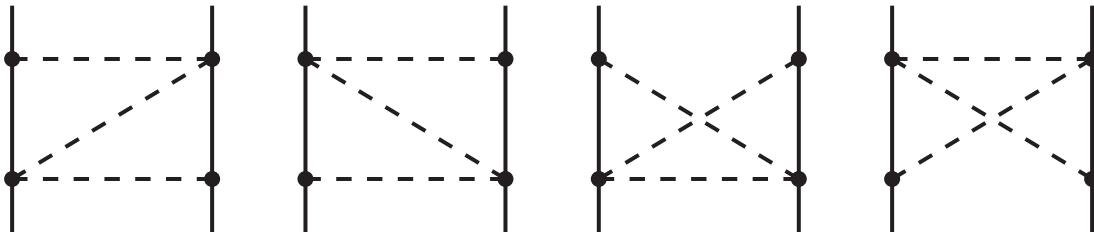


Fig.3: 3π -exchange diagrams of class III. The isoscalar NN-amplitudes sum up to zero.

Furthermore, we consider the diagrams of class III shown in Fig. 3. The isospin-factor of the first and second graph is $6 - 2 \vec{\tau}_1 \cdot \vec{\tau}_2$ while that of the third and fourth graph is $-6 - 2 \vec{\tau}_1 \cdot \vec{\tau}_2$.

Since all other factors occuring in these two types of diagrams are equal (modulo the sign of an $i0^+$ -term in one heavy nucleon-propagator which finally does not matter) one obtains only a contribution to the isovector spin-spin and tensor NN-amplitudes. Altogether, we find the following imaginary parts from the diagrams of class III,

$$\begin{aligned} \text{Im } W_S^{(III)}(i\mu) &= \frac{g_A^2}{18\mu^4(16\pi f_\pi^2)^3} \int_{2m_\pi}^{\mu-m_\pi} dw \sqrt{(w^2 - 4m_\pi^2)\lambda(w^2, m_\pi^2, \mu^2)} \\ &\quad \times [9w^4 - 5\mu^4 + 30\mu^2 m_\pi^2 - 9m_\pi^4], \end{aligned} \quad (20)$$

$$\begin{aligned} \text{Im } W_T^{(III)}(i\mu) &= \frac{2g_A^2}{9(16\pi f_\pi^2 \mu^2)^3} \int_{2m_\pi}^{\mu-m_\pi} dw \sqrt{(w^2 - 4m_\pi^2)\lambda(w^2, m_\pi^2, \mu^2)} \\ &\quad \times [4\mu^4 + 9\mu^2 m_\pi^2 + 9m_\pi^4 - 3w^4 + 6m_\pi^2(\mu^4 - m_\pi^4)w^{-2}]. \end{aligned} \quad (21)$$

In the chiral limit, $m_\pi = 0$, one has again potentials with a r^{-7} -dependence,

$$\widetilde{W}_T^{(III)}(r) = \widetilde{W}_S^{(III)}(r) = \frac{490g_A^2}{9(8\pi)^5 f_\pi^6} \frac{1}{r^7}, \quad (22)$$

and the asymptotic fall-off of these potentials for $r \rightarrow \infty$ is given by

$$\widetilde{W}_T^{(III)}(r) = \widetilde{W}_S^{(III)}(r) = \frac{g_A^2 m_\pi^3}{4\sqrt{3}(4\pi)^4 f_\pi^6} \frac{e^{-3m_\pi r}}{r^4} + \dots \quad (23)$$

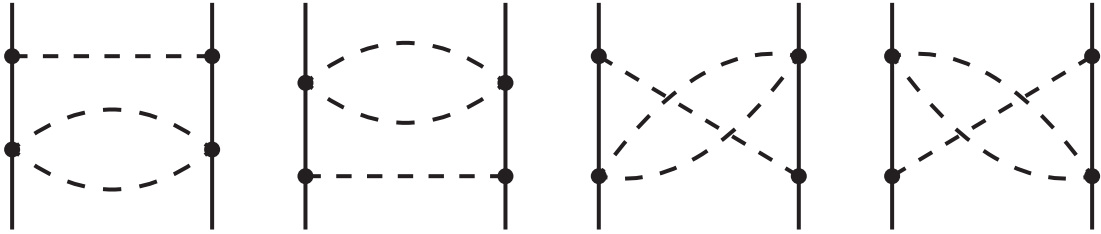


Fig.4: 3π -exchange diagrams of class IV. The symmetry factor of these graphs is $1/2$.

Finally, we consider the diagrams of class IV shown in Fig. 4. The isospin-factor of the first and second graph (planar boxes) is $6 - 4 \vec{\tau}_1 \cdot \vec{\tau}_2$ while that of the third and fourth graph (crossed boxes) is $6 + 4 \vec{\tau}_1 \cdot \vec{\tau}_2$. In ref.[1] it was shown that the irreducible part of the planar box and the crossed box are exactly equal up to a minus-sign. If one makes here use of this fact, one obtains again only a contribution to the isovector spin-spin and tensor NN-amplitudes from the diagrams of class IV. The explicit calculation of the corresponding imaginary parts leads to the following result,

$$\begin{aligned} \text{Im } W_S^{(IV)}(i\mu) &= \frac{g_A^2}{9\mu^4(16\pi f_\pi^2)^3} \int_{2m_\pi}^{\mu-m_\pi} dw \sqrt{(w^2 - 4m_\pi^2)\lambda(w^2, m_\pi^2, \mu^2)} \\ &\quad \times [9w^4 - 5\mu^4 + 30\mu^2 m_\pi^2 - 9m_\pi^4], \end{aligned} \quad (24)$$

$$\begin{aligned} \text{Im } W_T^{(IV)}(i\mu) &= \frac{g_A^2}{6(8\pi f_\pi^2 \mu^2)^3} \int_{2m_\pi}^{\mu-m_\pi} dw \sqrt{(w^2 - 4m_\pi^2)\lambda(w^2, m_\pi^2, \mu^2)} [w^4 + 7\mu^2 m_\pi^2 \\ &\quad - \frac{2}{3}\mu^4 - m_\pi^2(\mu^2 + m_\pi^2)^2 w^{-2} + 4m_\pi^2 \mu^4 (4m_\pi^2 - w^2) \lambda^{-1}(w^2, m_\pi^2, \mu^2)]. \end{aligned} \quad (25)$$

For the sake of completeness we give the corresponding NN-potentials in the chiral limit,

$$\widetilde{W}_T^{(IV)}(r) = -\frac{7}{3} \widetilde{W}_S^{(IV)}(r) = -\frac{140g_A^2}{3(8\pi)^5 f_\pi^6} \frac{1}{r^7}, \quad (26)$$

as well as their asymptotic behavior for $r \rightarrow \infty$, which reads

$$\widetilde{W}_T^{(IV)}(r) = \widetilde{W}_S^{(IV)}(r) = -\frac{g_A^2 m_\pi^3}{4\sqrt{3}(4\pi)^4 f_\pi^6} \frac{e^{-3m_\pi r}}{r^4} + \dots \quad (27)$$

The remaining chiral 3π -exchange diagrams (not considered here) carry an independent prefactor g_A^4/f_π^6 or g_A^6/f_π^6 . Since a larger number of nucleon-propagators is involved in these graphs one will be able to reduce the relevant 3π -phase space integrals only to double-integrals of the form $\iint_{z_2 < 1} d\omega_1 d\omega_2 \dots$ (see the calculation of $\text{Im } G_E^S(t)$ and $\text{Im } G_A(t)$ in ref.[7]). We hope to report on these remaining chiral 3π -exchange diagrams scaling with g_A^4 and g_A^6 in a future publication.

In Table 1, we present numerical results for the isovector spin-spin and tensor potentials generated by the 3π -exchange graphs of class I, II, III and IV for inter-nucleon distances $0.6 \text{ fm} \leq r \leq 1.4 \text{ fm}$, using the parameters $g_A = 1.32$, $f_\pi = 92.4 \text{ MeV}$ and $m_\pi = 138 \text{ MeV}$. If one would use instead the empirical nucleon axial-vector coupling constant $g_A = 1.267 \pm 0.004$ [8] the numerical values would decrease by about 8%. One observes that the repulsive isovector spin-spin and tensor potentials coming from the complete class I are much smaller than the corresponding ones found in ref.[3] due to cancelations between different diagrams of class I. The repulsive isovector spin-spin and tensor potentials due to class I are actually overcompensated by more attractive ones coming from class II. Interestingly, for class III the isovector spin-spin and tensor potential are equal, i.e. $\widetilde{W}_S^{(III)}(r) = \widetilde{W}_T^{(III)}(r)$. This relation is not obvious from the spectral representations eqs.(10,11) and the imaginary parts given in eqs.(20,21). In all other cases one finds that the tensor potential is larger in magnitude than the spin-spin potential. Note that the tensor potentials due to class III and class IV cancel each other almost completely. The absolute strengths of the 3π -exchange potentials calculated here are less than 0.6 MeV for distances $r \geq 0.8 \text{ fm}$ followed by a very fast exponential fall-off and thus they are completely negligible in comparison to the 2π -exchange potentials (see e.g. refs.[1, 5]). One also notices that the numerical values of the 3π -exchange potentials at $r = 1.4 \text{ fm}$ deviate still strongly from that ones given by the ($r \rightarrow \infty$)-asymptotics, eqs.(15,19,23,27). In particular the spin-spin and tensor potentials due to classes I, II, IV are far from being approximately equal. Similar features were also found in ref.[3] (see Fig. 5) and there the ($r \rightarrow \infty$)-asymptotics turned out to be accurate on the 20% level only for $r \geq 4 \text{ fm}$. The ($r \rightarrow \infty$)-asymptotics is therefore of no use to get a reasonable numerical estimate of the chiral 3π -exchange potentials for $r \leq 1.5 \text{ fm}$.

Furthermore, because of the finite size of the nucleon one can probably trust a calculation based on point-like nucleons and pions only for distances $r \geq 1 \text{ fm}$. Moreover, one can expect that the other chiral 3π -exchange diagrams not calculated here will produce NN-potentials larger by at most a factor $g_A^4 \simeq 3$. Such potentials would be still much too small in order to be of any practical relevance. One may therefore conclude that the effects due to uncorrelated (chiral) 3π -exchange in the NN-interaction are all negligibly small. The resonant 3π -exchanges in form of $\omega(782)$ - and $a_1(1260)$ -exchange seem to be the dominant effects. For example, the static isovector spin-spin and tensor potentials due to $a_1(1260)$ -exchange,

$$\widetilde{W}_S^{(a_1)}(r) = -\frac{g_{a_1 N}^2}{6\pi r} e^{-m_a r}, \quad \widetilde{W}_T^{(a_1)}(r) = \frac{g_{a_1 N}^2}{12\pi r} e^{-m_a r} \left(1 + \frac{3}{m_a r} + \frac{3}{m_a^2 r^2}\right), \quad (28)$$

are about one order of magnitude larger than typical chiral 3π -exchange potentials (see Table 1). The same holds for the total sum of the isovector spin-spin and tensor potentials due to the four classes of diagrams evaluated here. In order to obtain the values of $\widetilde{W}_{S,T}^{(a_1)}(r)$ given in Table 1 we used the central value of the a_1N -coupling constant $g_{a_1N}^2/4\pi = 7.3 \pm 3.0$ as derived from forward NN-dispersion relations in ref.[9]. The extreme smallness of the chiral 3π -exchange NN-potential found here is in agreement with the results of ref.[7]. There it was shown that the 3π -continuum makes only a negligibly small contribution to the spectral-functions of the isoscalar electromagnetic and isovector axial form factors of the nucleon and a few vector-meson poles give therefore a sufficiently accurate representation of these spectral-functions. As it could be expected the same features apply to the NN-potential.

r [fm]	0.6	0.7	0.8	0.9	1.0	1.1	1.2	1.3	1.4
$\widetilde{W}_S^{(I)}$ [keV]	146	38.6	11.5	3.69	1.24	0.43	0.14	0.04	0.01
$\widetilde{W}_T^{(I)}$ [keV]	1591	476	164	62.6	26.0	11.6	5.43	2.67	1.37
$\widetilde{W}_S^{(II)}$ [keV]	-2372	-736	-262	-104	-44.5	-20.4	-9.88	-5.00	-2.63
$\widetilde{W}_T^{(II)}$ [keV]	-4616	-1405	-491	-191	-80.5	-36.3	-17.3	-8.63	-4.47
$\widetilde{W}_S^{(III)}$ [keV]	5121	1631	596	242	107	50.1	24.8	12.9	6.93
$\widetilde{W}_T^{(III)}$ [keV]	5121	1631	596	242	107	50.1	24.8	12.9	6.93
$\widetilde{W}_S^{(IV)}$ [keV]	1295	372	121	43.0	16.3	6.49	2.64	1.07	0.43
$\widetilde{W}_T^{(IV)}$ [keV]	-4729	-1518	-559	-228	-101	-47.6	-23.7	-12.3	-6.63
$\widetilde{W}_S^{(tot)}$ [keV]	4190	1306	467	185	80.0	36.6	17.7	9.01	4.74
$\widetilde{W}_T^{(tot)}$ [keV]	-2633	-816	-290	-114	-48.5	-22.2	-10.8	-5.36	-2.80
$\widetilde{W}_S^{(a_1)}$ [MeV]	-37.71	-15.71	-7.26	-3.41	-1.62	-0.78	-0.38	-0.18	-0.09
$\widetilde{W}_T^{(a_1)}$ [MeV]	34.49	14.31	6.18	2.75	1.25	0.58	0.27	0.13	0.06

Tab.1: Isvector spin-spin and tensor NN-potentials due to the chiral 3π -exchange graphs of classes I, II, III, IV (shown in Figs. 1, 2, 3, 4) versus the nucleon distance r . Note that the units for these potentials are keV. The total sums of potentials due to these four classes are denoted by $\widetilde{W}_{S,T}^{(tot)}$. The static $a_1(1260)$ -exchange spin-spin and tensor NN-potentials are instead given in units of MeV.

References

- [1] N. Kaiser, R. Brockmann and W. Weise, *Nucl. Phys.* **A625**, 758 (1997) and refs. therein.
- [2] M.C.M. Rentmeester, R.G.E. Timmermans, J.L. Friar and J.J. de Swart, *Phys. Rev. Lett.* **82**, 4992 (1999).
- [3] J.C. Pupin and M.R. Robilotta, *Phys. Rev.* **C60**, 014003 (1999).
- [4] S. Weinberg, *Phys. Rev.* **166**, 1568 (1968).
- [5] N. Kaiser, S. Gerstendörfer and W. Weise, *Nucl. Phys.* **A637**, 395 (1998).
- [6] V. Bernard, N. Kaiser and U.G. Meißner, *Phys. Lett.* **B332**, 415 (1994); *Nucl. Phys.* **B457**, 147 (1995).
- [7] V. Bernard, N. Kaiser and U.G. Meißner, *Nucl. Phys.* **A611**, 429 (1996).
- [8] Review of Particle Physics, *Eur. Phys. J.* **C3**, 662 (1998).
- [9] W. Grein and P. Kroll, *Nucl. Phys.* **A338**, 332 (1980).